Assessment of soil contamination around an abandoned mine in a semi-arid environment using geochemistry and geostatistics: Pre-work of geochemical process modeling with numerical models

A. Khalil [a,*], L. Hanich [a], A. Bannari [b], L. Zouhri [c], O. Pourret [c], R. Hakkou [d]

[a] Geo-resources Laboratory, associated Unit to CNRST (URAC42), Department of Earth Sciences, Faculty of Sciences and Technology Guéliz, Cadi Ayyad University, Abdelkarim Elkhattabi Avenue, Gueliz, P.O. Box 549, Marrakech, Morocco
[b] Department of Geography, University of Ottawa, Ottawa (Ontario), Canada K1N 6N5
[c] HydrISE, Institut Polytechnique LaSalle Beauvais, 19 rue Pierre Waguet, F-60026 Beauvais Cedex, France
[d] LCME, Faculté des Sciences et Techniques Guéliz, Cadi Ayyad University, Abdelkarim Elkhattabi Avenue, Gueliz, P.O. Box 549, Marrakech, Morocco

ARTICLE INFO

ABSTRACT

One of the most serious environmental issues related to mining industry in Morocco and elsewhere around the world, is the pollution from abandoned mine sites. Mine wastes cause obvious sources of soil contaminations. Climatic effects such as heavy rainfall engender metal dispersion in semi-arid areas, since soils are typically and scarcely vegetated. In this study, extension and magnitude of soil contaminations with toxic elements from abandoned Kettara mine, in Morocco, are assessed using geochemical analysis and geostatistics for mapping. Soils and mine wastes are sampled and analyzed for 41 chemical elements (Mo, Cu, Pb, Zn, Ag, Ni, Co, Mn, Fe, As, U, Au, Th, Sr, Cd, Sb, Bi, V, Ca, P, La, Cr, Mg, Ba, Ti, Al, Na, K, W, Zr, Ce, Sn, Y, Nb, Ta, Be, Sc, Li, S, Rb and Hf). Based on enrichment factor (EF), only five elements of interest (Cu, Pb, Zn, As, and Fe) were selected in this research. Geochemical background is determined with exploratory data analysis and geochemical maps were elaborated using geostatistics in Geographic Information System (GIS) environment.

The obtained results show that Kettara soils are contaminated with metals and metalloid that exceed the established geochemical background values (Cu ≈ 43.8 mg/kg, Pb ≈ 21.8 mg/kg, Zn ≈ 102.6 mg/kg, As ≈ 13.9 mg/kg and Fe ≈ 56,978 mg/kg). Geochemical maps show that the deposited mine wastes are responsible for soil contaminations with released metals and metalloid that have been dispersed downstream from the mine waste mainly, through water after rainfall. For sustainable development and environmental planning, the current study is expected to serve as a reference for politicians, managers, and decision makers to assess soil contaminations in abandoned mine sites in Morocco.

© 2012 Elsevier B.V. All rights reserved.

1. Introduction

Acid Mine Drainage (AMD) from mine waste and contaminations of soils and water with metals are considered as major environment problems in mining areas (U.S. Bureau of Mines, 1994). This environment phenomenon is produced with oxidation of sulfide minerals e.g. pyrite and pyrrhotite (Bussiere, 2009; Hakkou et al., 2008a). Consequently, acidification would increase the dissolution of toxic metals from tailings, waste rock piles, and open pits. Therefore, soil and water ecosystem will be contaminated (Bell and Donnelly, 2006; Sams and Beer, 2000). Certainly, as rainfall water infiltrates into the underground soil/rock, it can cause pore-water flow in the pore space of the soil/rock. The resulting pore-water flow can be advective or convective (Zhao et al., 2004, 2008a) depending on geological conditions of the mine site. When the

pore-water becomes in contact with the soil/rock, it can react chemically with the mine waste dissolving heavy metals at the mine site. Since the dissolved heavy metals can be transported in the soil/rock through pore-water advection, convection and solute diffusion/dispersion (Zhao et al., 2007), they can contaminate both the land and the groundwater at the mine site. In addition, as demonstrated theoretically, the dissolved metal front may become unstable when it propagates in the soil/rock at the mine site (Zhao et al., 2008b, 2010a). This is the scientific problem, known as the mine site contamination, which is the focus of this study.

With the stimulus of exploring giant ore deposits in the deep earth, extensive and systematic work has been conducted to develop advanced computational methods and algorithms for simulating physical and chemical processes associated with ore body formation and mineralization within the Earth's crust (Zhao et al., 2009, 2010b). As a result, a new emerging discipline, known as the computational geosciences (Zhao et al., 2009), has been established. Due to mathematical similarity, the advanced computational methods and algorithms (Zhao et al.,

2006, 2009) can be also used to solve mine site contamination problems if the geological and the geochemical data are available at the mine site. From this point of view, the scientific significance of this study can be described as follows. First, detailed geochemical data produced in this study can be used as an example to extend the advanced computational methods and algorithms to the computational simulation of mine site contamination problems. This will answer how and why the mine site is contaminated in a scientific manner. Second, advanced computational methods and algorithms are then used to develop techniques to remove heavy metals from the contaminated mine site, which is known as the mine site remediation problem (Zhao et al., 2012) and has great practical significance in the current world.

Furthermore, knowledge of soil geochemistry is fundamental when we attempt to determine the effects stemming from an anthropogenic activity and its impact on the geo-ecosystems as a result of its toxicities (Albanese et al., 2007; Cicchella et al., 2005; Giaccio et al., 2012; Guillén et al., 2011, 2012). In this respect, it is essential to establish geochemical maps for chemical elements associated with different lithologies in order to distinguish if their source is geogenic or anthropogenic (Plant et al., 2001). In addition of the scientific or mining standpoint, geochemical maps constitute an effective tool for environmental planning (Ferguson and Kasamas, 1999; Li et al., 2004). They reveal information about source, distribution, and dynamics of chemical elements. Geochemical maps include both the geogenic concentration or geochemical background (GB) value, and the concentration that is the result of anthropogenic activity (Guillén et al., 2011). This explains why GB defined by Hawkes and Webb (1962) as "*the normal abundance of a chemical element in barren earth material*" has become crucial in environmental studies. It was introduced to differentiate between normal and abnormal element concentration (Martínez et al., 2007). Exploratory Data Analysis (EDA) has been recommended as an effective tool to determine the GB (Zhou and Xia, 2010). According to the literature, this method was tested and proved by numerous authors (Bounessah and Atkin, 2003; Reimann et al., 2005).

Finally, GIS based on geostatistical analysis is one of the most important tools for studying environmental geochemistry problems (Acosta et al., 2011). It provides an effective means for researching the spatial variability of pollutants (Sun et al., 2012). Geostatistics is an advanced methodology that facilitates quantification of the spatial features of soil parameters and enables spatial interpolation (Carlon et al., 2001; Zhang et al., 2000). According to the literature, numerous authors have used kriging analysis in GIS environment to elaborate geochemical maps to quantify both extension and magnitude of contamination with toxic elements (García-Lorenzo et al., 2012; Li and Feng, 2012; Li et al., 2004; Nakayama et al., 2011).

The abandoned Kettara mine site (Morocco) was selected to analyze the impact of mining activity on the surrounding soils. The objectives of this study were as follows: 1) geochemical characterization of Kettara soils and tailings; 2) determination of GB values of selected chemical elements in Kettara soils; and 3) elaboration of geochemical maps regarding the selected toxic elements and their comparison with the elaborated GB to reveal the degree of pollution of the Kettara mine site surrounding soils and to examine possible health risks.

2. Materials and methods

2.1. Study site

The abandoned Kettara mine is located approximately 35 km northwest of Marrakech city in the core of the central Jebilet Mountains (Fig. 1). According to the latest governmental census (2004), the population of Kettara village is approximately 2000 people. The climate of this region is classified as semi-arid environment with average maximum and minimum temperature ranging from 12 °C in January to 29 °C in July, respectively. The average annual rainfall is 250 mm. The potential evapotranspiration rate surpasses 2500 mm/year. NE–SW

wind flow is prevailing in the study site (ONEM, 1997). Perennial streams do not exist and surface water consists of ephemeral watercourses that are operational only during rainfall events.

The Kettara mine had undergone three mine exploitation phases. In the first phase, between 1938 and 1962, the iron oxide was extracted from the iron hat "gossans" to produce red oxide (50 to 58% of Fe) for paint industry. In the second phase, between 1955 and 1966, the zone of cementation was exploited for pyrite (180,000 t with 38 wt.% of sulfide) (Huvelin, 1977). During these two phases the ores were delivered in their raw state without any mineralogical concentration, and the mine wastes were about 1 million ton (Mt) of coarse waste rocks. In the third and final phase, between 1964 and 1981, the mine produced more than 5.2 Mt of pyrrhotite concentrate containing an average of 29 wt.% sulfide. The pyrrhotite was extracted from the ore by gravimetric separation (jigs). This ore enrichment process generated a wide range of particle size fractions in the mine wastes (jigs refuse materials). These latter can be divided into two broad classes of materials: coarse mine wastes (fine gravel) and fine mine wastes (silt). Throughout this period, more than 3 Mt of mine wastes were stockpiled over an area of about 30 ha (Fig. 2). The Kettara wastes contain 1.6 to 14.5 wt.% sulfur, mainly sulfide minerals (e.g., pyrrhotite, pyrite, chalcopyrite, galena, and sphalerite) (Hakkou et al., 2008a). The Kettara mine wastes have produced significant amounts of AMD. Previous researches (Hakkou et al., 2008b) have shown that effluent water samples had low pH (2.9 to 4.2), and high concentrations of sulfate (from 47 to 5000 mg/L) and iron (from 1 to 1200 mg/L). Furthermore, the Cu and Zn concentrations had reached 58 and 45 mg/L, respectively. At the Kettara mine site, several secondary minerals have been observed at the surface (e.g., goethite, jarosite, alunite, gypsum). The presence of these minerals in large quantities shows that AMD generation is very active at Kettara (Hakkou et al., 2008a).

The Kettara sulfide deposit is a typical example of metamorphosed deposits hosted by Visean volcano-sedimentary formations. The mineralized body consists of major and minor lenses of massive pyrrhotite, with small amounts of sphalerite, galena, chalcopyrite, pyrite, arsenopyrite and glaucodot. The structure resulted from an intra-Westphalian tectono-metamorphic phase of the Hercynian orogeny (Hibti et al., 1999). The substrate of Kettara is composed of fractured and altered shale, which facilitates AMD infiltration. Furthermore, the principal groundwater table is located in this formation and has a depth of between 10 m and 20 m. According to Lghoul et al. (2012), groundwater sampled at Kettara mine site from wells located downstream of the mine wastes is contaminated by the AMD, mainly by sulfates (>1200 mg/L) and presents high conductivity values, 3000 to 3680 μS/cm.

2.2. Sampling and samples preparation

Special consideration was given to the used criteria to select sampling points' locations. After a review of topographic and geologic maps, and according to previous studies on the abandoned Kettara mine (Hakkou et al., 2008a; Khalil et al., 2011), soil sampling was established in 3 different areas based on the location of the mine wastes. The sampling design was made to compare concentration gradient and possible chemical element mobilization. The distance between sampling points varies from 150 to 350 m. Four groups of soil samples have been collected: 1) samples located upstream of the mine waste (13 samples); 2) samples located nearby the mine waste (27 samples); 3) samples located downstream of the mine site (22 samples); and 4) mine waste samples from the Kettara mine tailings (12 samples). Finally, 62 soil samples (from S1 to S62) and 12 mine waste samples (from R1 to R12) were collected within the study site, approximately 6 km² (Fig. 2). Geographic coordinates of sampling points were measured using a Global Positioning System (GPS) within ±5 m accuracy, with the "Lambert North Morocco" map projection.
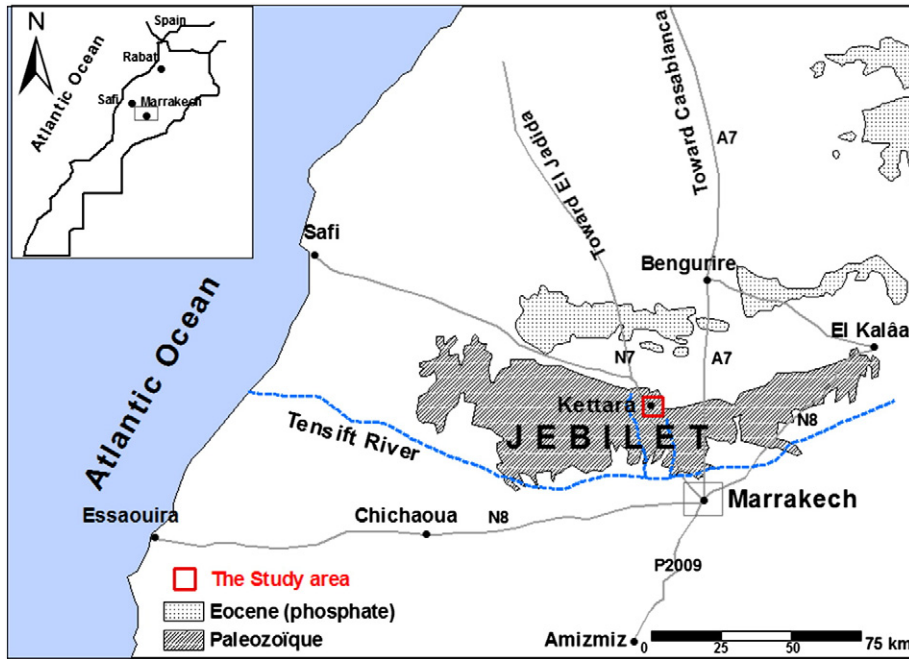
Fig. 1. Geographical location of the study site.

Samples were taken within the first 20 cm of soil using a stainless steel shovel. To minimize sampling errors, each sample underwent a quartering operation, photographed with a digital camera, and then stored in a polyethylene bag. After this step, each sample was dried in an oven at 100 °C in the laboratory and then sieved through a 2 mm mesh. The total sample under 2 mm was ground in agate mortar until a fraction smaller than 63 μm for subsequent chemical analysis.

2.3. Chemical analysis

Chemical analyses were carried out at Acme Analytical Laboratories Ltd. (Vancouver, Canada), accredited under ISO 9002. The considered analyzed elements are Mo, Cu, Pb, Zn, Ag, Ni, Co, Mn, Fe, As, U, Au, Th, Sr, Cd, Sb, Bi, V, Ca, P, La, Cr, Mg, Ba, Ti, Al, Na, K, W, Zr, Ce, Sn, Y, Nb, Ta, Be, Sc, Li, S, Rb and Hf. Soil samples were digested using a strong multi-acid method that dissolves most minerals. Then, 0.25 g split
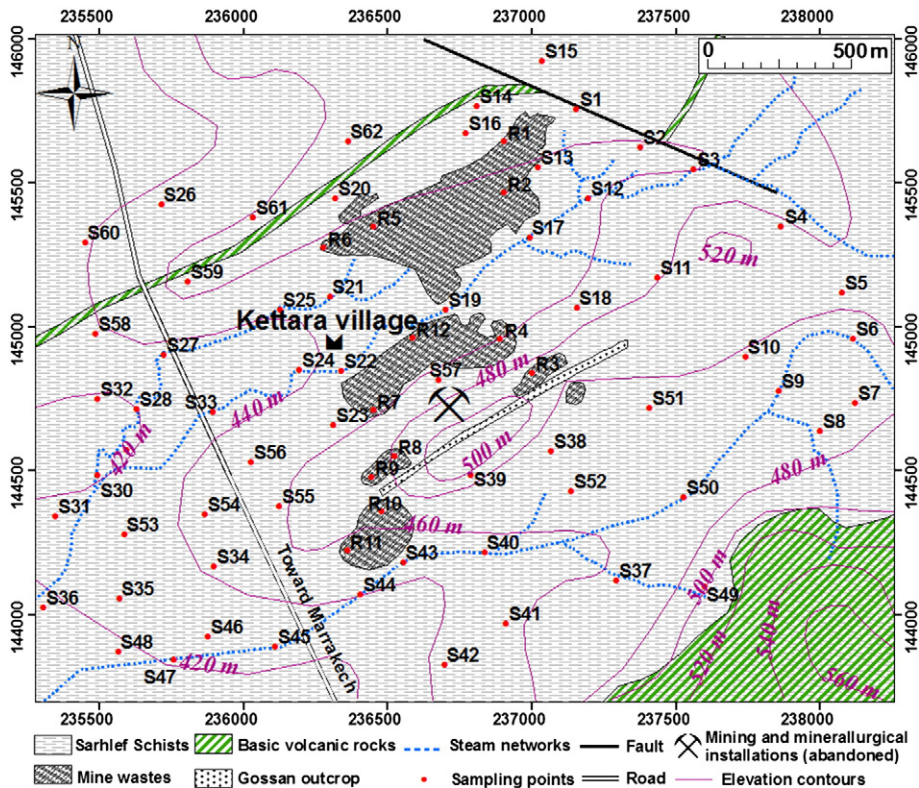

Fig. 2. Geological map of the study site and sampling point locations.

was heated in HNO_3–$HClO_4$–HF to fuming and taken to dryness. The residue was further dissolved in HCl. Then, solutions were analyzed using Inductively Coupled Plasma Mass Spectrometry (ICP-MS).

The data quality was assessed using duplicate sample analyses, blanks, and concentration measurement accuracy estimation. This latest was achieved based on repeated analyses of multi-element soil standard "OREAS 45c" prepared from a 50:50 blend of barren soil, and soil characterized by anomalous levels of precious and base metals. The anomalous sample was obtained from soil developed over a Ni–Cu–PGE mineralized contact between gabbro and pyroxenite from the Southern Murchison region of Western Australia. While, the barren sample was taken from an in situ layer of mature soil developed over early tertiary olivine basalt in outer eastern Melbourne, Victoria, Australia. According to data quality result assessment, the concentration measurement accuracy was estimated at ±5% for all the considered elements. Finally, analytical results of blank solutions showed that all the elements of interest are below the detection limits.

2.4. Statistical analysis

2.4.1. Descriptive statistics

The following statistical parameters were determined for the 41 elements considered and analyzed: minimum, maximum, mean and median for the central tendency measurement, standard deviation and variation coefficient for the data dispersion measurement; while the data distribution was tested for normality using Kolmogorov–Smirnov (K–S) test, kurtosis and skewness (Tables 1 and 2). These parameters will be helpful for comparing datasets, therefore summarizing the obtained results and facilitating its subsequent interpretation (Burgos et al., 2005; Cai et al., 2012; Martínez et al., 2007).

2.4.2. Enrichment factors

In order to select chemical elements that have been enriched in Kettara soils, enrichment factor (EF) was calculated (Bourennane et al., 2010; Li and Feng, 2012; Martínez et al., 2007). The concept of EF was developed in the early seventies to derive the origin of elements in the atmosphere, precipitation or seawater, and was progressively applied to other environmental materials such as soils, lake sediments or peat (Bourennane et al., 2010; Reimann et al., 2005). It was widely employed to identify the anthropogenic source of metallic elements (Li and Feng, 2012). Based on EF, five contamination categories were recognized: 1) EF < 2 states deficiency to minimal enrichment; 2) 2 ≤ EF < 5 moderate enrichment; 3) 5 ≤ EF < 20 significant enrichment; 4) 20 ≤ EF ≤ 40 very high enrichment, and; 5) EF > 40 extremely high enrichment (Han et al., 2006; Lu et al., 2009a,b). The EF was calculated for the chemical elements using the following generalized equation according to Chester and Stoner (1973) and Zoller et al. (1974):

$$EF_{El} = \frac{[El]_{sample}/[X]_{sample}}{[El]_{crust}/[X]_{crust}}$$

where "*El*" is the element under consideration, the square brackets indicate concentration (usually in mass/mass units, such as mg/kg), "*X*" is the chosen reference element (see below) and the subscripts "sample" or "crust" indicate which medium concentration refers to. Crust refers to Clarke of Earth's crust, most often continental or Upper Continental Crust (UCC). The Clarke values corresponding to mean concentration of chemical elements in the UCC were given by McLennan (2001). In this study, Aluminum was selected to be the reference value. Indeed, Al is the most common reference value used to calculate the EF (Bourennane et al., 2010; Buat-Menard and Chesselet, 1978; Lu et al., 2009a).

Table 1 summarizes EF values which indicate how many times measured concentrations exceed the Clarke values.

2.4.3. Exploratory Data Analysis (EDA)

In addition to the statistical and EF analyses, the EDA technique was assessed because it is an appropriate technique for identifying anthropogenic influences (Zhou and Xia, 2010). EDA was applied to determine the GB of soil. This latter will serve as a reference to assess the soil contamination by toxic elements. EDA consists of elaborating graphs such as histograms with the distribution curves, box plots also called a box-and-whiskers plot, in which six parameters are described (lower limit, first quartile, median, third quartile, upper limit and extreme values), and normal Quantile–Quantile plots (Q–Q plots) which were applied to look for different intervals of toxic element concentrations which imply likely the presence of different processes or multiple population (Zhou and Xia, 2010). In addition, the EDA will provide a better observation of the shape of the distribution values (Martínez et al., 2007).

2.5. Geochemical mapping and multi-criteria analysis using GIS

The coordinate locations of sampling soils and the concentration values of selected chemical elements were intergraded in a GIS database. Spatial interpolation and mapping were carried out for the target elements using geostatistics. This consisted of complex semi-variograms for each considered elements (Cu, Pb, Zn, As and Fe). Both ordinary and simple kriging were tested considering different mathematical models for adjustment. According to Li et al. (2001), the optimized model should minimize standard mean (close to 0), and the standard root mean square error (RMSE) should be closest to 1. Iterative testing concluded that exponential model provided the best adjustment with excellent RMSE values. In addition, similar accuracies were obtained with ordinary and simple kriging. Consequently, only the latest was selected in this study. The theoretical semi-variogram model values and error estimation are summarized in Table 3.

Multi-Criteria Analysis (MCA) using GIS was applied on derived geochemical maps in order to elaborate a risk map of soil contamination. This map was established using the spatial analyst of Arc GIS software conducting queries on the geochemical map of each considered elements (ESRI, 2012). Each query extracts only the areas characterized with highly anomalous content of toxic elements (hot spots). Areas where metallic and metalloid content exceeds 300 mg/kg for Cu, 100 mg/kg for Pb, 300 mg/kg for Zn, 50 mg/kg for As and 100,000 mg/kg for Fe were extracted. Finally, those areas were overlaid to establish the risk map of contaminated soils which will be so informative for politicians and decision makers (Komnitsas and Modis, 2006).

3. Results and discussion

3.1. Statistical analysis

The EF analysis shows five different classes. The first class considers the elements with minimal enrichment and it includes the following elements: Mo, Ni, Co, Mn, U, Th, Sr, V, Ca, P, La, Cr, Mg, Ba, Ti, Al, Na, K, W, Zr, Ce, Sn, Y, Nb, Ta, Be, Sc, Rb, and Hf. The second class considers elements with moderate enrichment and it includes the following elements: Pb, Zn, Ag, Fe, Cd and Li. The third class considers elements with significant enrichment and it includes Sb and Cu. The fourth class considers elements with high enrichment and it includes As and Bi. Finally, the fifth class, which corresponds to elements with extremely high enrichment, includes only Au (Table 1). Although the following elements: Ag, Cd, Bi, Sb, Li, and Au have an EF ranging from 2.93 to 70.09, their concentrations in the Kettara soils are extremely low. Their mean concentrations are 0.13 mg/kg, 0.32 mg/kg, 2.52 mg/kg, 1.57 mg/kg, 42.45 mg/kg, and 0.11 mg/kg, for Ag, Cd, Bi, Sb, Li, and Au, respectively (Table 1). These low concentrations would not have any adverse effects on humans or animals in Kettara area. However, the elements Cu, Pb, Zn As, and Fe have an EF ranging from 2.17 to 25.17 and their concentrations in Kettara soils are high with a

Table 1
Descriptive statistics, Clarke values (a) and enrichment factors of the chemical elements of the examined Kettara soils.

Elements	Minimum	Maximum	Mean	Median	SD	VC	Skewness	Kurtosis	K–S test	Upper Continental Crust Clarke values[a]	Enrichment factor (Upper Continental Crust)
Mo	0.3	4.7	1.13	0.8	0.86	0.76	2.31	5.81	0.000	1.50	0.86
Cu	20.6	1687	203.38	62.3	308.32	1.52	2.82	9.25	0.000	25	9.22
Pb	7.6	207.8	41.44	32.9	32.57	0.79	3.25	12.97	0.000	17	2.76
Zn	62	449	135.95	116.5	62.96	0.46	2.51	9.22	0.000	71	2.17
Ag	0.1	0.9	0.13	0.1	0.14	1.06	3.46	16.40	0.000	0.05	2.93
Ni	4	246.3	56.23	46.2	36.19	0.64	3.13	12.85	0.000	44	1.45
Co	13.6	64.2	27.47	24.2	9.80	0.36	1.80	4.54	0.003	17	1.83
Mn	134	2170	911.90	886	338	0.37	0.76	2.18	0.200	600	1.72
Fe	43,300	374,900	76,974	59,800	53,268	0.69	3.62	16.21	0.000	35,000	2.49
As	6	124	33.31	25	26.13	0.78	1.87	3.19	0.000	1.5	25.17
U	0.5	2.3	1.53	1.6	0.37	0.24	−0.35	0.21	0.029	2.8	0.62
Au	0.1	0.6	0.11	0.1	0.07	0.67	6.60	46.62	0.000	0.0018	70.09
Th	2.2	15.8	10.86	11.4	2.99	0.28	−1.00	0.83	0.035	10.70	1.15
Sr	8	156	79.15	76.0	23.29	0.29	0.27	1.81	0.200	350	0.26
Cd	0.1	0.8	0.32	0.3	0.13	0.40	1.13	2.93	0.000	0.10	3.66
Sb	0.5	5.3	1.57	1.1	1.13	0.72	1.74	2.45	0.000	0.20	8.92
Bi	0.05	30.4	2.58	0.5	5.41	2.10	3.48	13.52	0.000	0.13	23.06
V	44	281	140.40	135.5	34.71	0.25	1.34	4.94	0.002	107	1.49
Ca	1300	73,700	13,813	10,300	13,295	0.96	2.23	6.41	0.000	30,000	0.52
P	220	1450	752.58	725	207.77	0.28	0.69	2.06	0.017	700	1.22
La	8	48.4	33.82	35.7	8.27	0.24	−0.80	0.80	0.069	30	1.28
Cr	25	1081	134.97	91.0	145.19	1.08	5.09	30.66	0.000	83	1.84
Mg	2800	43,800	15,944	13,300	7857	0.49	1.94	4.09	0.000	13,300	1.36
Ba	65	652	407.55	436.0	116.22	0.29	−0.89	0.92	0.000	550	0.84
Ti	610	18,340	5512	4920	2403	0.44	2.53	12.57	0.001	4100	1.52
Al	11,600	89,900	70,923	72,850	10,617	0.15	−3.10	15.48	0.000	80,400	1.00
Na	530	14,140	5725	5505	2153	0.38	1.75	6.12	0.000	28,900	0.22
K	2800	24,700	18,140	19,450	4899	0.27	−1.10	0.85	0.003	28,000	0.73
W	0.4	2.7	1.44	1.4	0.45	0.31	0.79	1.10	0.000	2	0.82
Zr	22.4	108.5	87.32	92.6	16.17	0.19	−1.39	2.95	0.003	190	0.52
Ce	17	102	72.52	76.5	18.11	0.25	−0.78	0.53	0.067	64	1.28
Sn	1.5	6.6	3.10	2.9	0.75	0.24	1.98	7.23	0.000	6	0.64
Y	2.8	49.1	20.26	19.6	6.74	0.33	1.05	4.74	0.200	22	1.04
Nb	2.4	21.8	12.64	13.4	3.62	0.29	−0.46	0.16	0.200	12	1.19
Ta	0.1	1.5	0.85	0.9	0.25	0.30	−0.42	0.36	0.004	1	0.96
Be	1	3	1.98	2.0	0.68	0.34	−0.35	0.11	0.000	3	0.74
Sc	3	30	15.76	15.0	4.44	0.28	0.92	2.56	0.000	14	1.31
Li	4.7	66.9	42.45	41.1	10.08	0.24	−0.30	2.77	0.070	20	2.41
S	1000	53,000	4073	1000	9742	2.39	3.50	13.07	0.000	*	*
Rb	13.9	118.4	80.94	85.7	23.36	0.29	−0.73	−0.12	0.017	112	0.82
Hf	0.7	3.6	2.58	2.7	0.50	0.20	−1.06	1.99	0.000	5.80	0.50

[a] Clarke values = mean concentrations of the chemical elements in the upper continental crust (UCC) given by McLennan (2001); Geochemical data are expressed in mg/kg; VC = variation coefficient; SD = standard deviation.

mean concentration of 203.38 mg/kg, 41.44 mg/kg, 135.95 mg/kg, 33.31 mg/kg, 769.74 mg/kg, for Cu, Pb, Zn As, and Fe, respectively (Table 1). The Cu, Pb, Zn As, and Fe were selected as elements with important interest because they are related to mineral paragenesis and therefore, to mining and mineralogical activities in Kettara. Furthermore, they are known to be toxic and hazardous at high concentrations (Chowdhury et al., 2000; Davies and Mundalamo, 2010; Gurzau et al., 2003; Lockitch, 1993; Peplow and Edmonds, 2005).

The Cu, Pb, Zn, As, and Fe concentration levels ranged from 20.6 to 1687 mg/kg, from 7.6 to 207.8 mg/kg, from 62 to 449 mg/kg, from 6 to 124 mg/kg and from 43,300 to 374,900 mg/kg, respectively. The mean concentrations are 203.38 mg/kg, 41.44 mg/kg, 135.95 mg/kg, 33.31 mg/kg and 76,974 mg/kg, for Cu, Pb, Zn, As and Fe respectively (Table 1). These concentrations disclose that the metallic and metalloid content in the Kettara soil is high. In order to reveal if the origin of this content is weather geogenic or anthropogenic and for a better observation of the value distribution shape, Figs. 3, 4 and 5 illustrate graphs (histograms, box plots and Q–Q plots for the selected elements) obtained from EDA. Fig. 3a to e shows that all histograms are asymmetric and right-skewed. Skewness characterizes the distribution asymmetry degree around its mean (Zhou and Xia, 2010). The skewness feature of Cu, Pb, Zn, As, and Fe concentrations suggests that the majority of the samples are located in the lowest intervals of concentration. Fig. 4a to e shows that all the boxes are displaced towards the minimum

concentration values. This confirms the fact that the concentration distribution of selected elements is skewed. Numerous outliers (anomalous values above the upper limit of the box plots) of Cu, Pb, Zn, As, and Fe are shown in the box plots (Figs. 4a to 5e). Outliers are indicators of unusual processes. They usually exist in mineralized region or in contaminated sites (Zhou and Xia, 2010). According to Figs. 2 and 4, the outliers of selected elements are located nearby and downstream of the mine wastes which, are the likely source of the anomalous metallic and metalloid content. Fig. 5 shows the Q–Q plots of selected elements. The measured values are plotted on the X axis and the expected values under a normal distribution are plotted on the Y axis. Q–Q plots provide a powerful visualization of the data which shows inflection points that imply the likely presence of different processes (Zhang et al., 2008; Zhou and Xia, 2010). The plots of selected elements (Fig. 5a to e) undergo inflection points and they are far from the theoretical normal slop. This implies that the selected element concentration distribution is asymmetric. Furthermore, the large standard deviation, variation coefficient, skewness, and kurtosis calculated for each selected elements (Table 1) imply that these elements have asymmetric distributions with a long tail to the right which suggest the presence of high extreme values and, consequently, high degree of pollution. Asymmetries are also reflected by the numerical test of normality Kolmogorov–Smirnov (K–S test) that gives values of zero for all the selected elements which indicates that the concentration values are not normally distributed (Chen et al.,

Table 2
Descriptive statistics of chemical elements of the examined Kettara mine wastes.

Elements	Minimum	Maximum	Mean	Median	SD	VC	Skewness	Kurtosis
Mo	1	13.70	4.14	2.80	3.52	0.85	2.24	5.05
Cu	879	6971	2428	1508	1974	0.81	1.76	2.02
Pb	7	778	156	81	217	1.39	2.53	6.79
Zn	79	361	176	153	83	0.47	1.22	1.11
Ag	0.10	13.10	1.67	0.65	3.62	2.16	3.40	11.70
Ni	2.50	48.90	14.32	9.30	14.53	1.01	1.50	1.78
Co	14	313	67	36	85	1.27	2.63	7.41
Mn	132	879	377	282	255	0.68	0.99	−0.33
Fe	90,200	413,600	294,825	307,650	91,925	0.31	−0.98	1.00
As	13	715	200	109	212	1.06	1.78	2.47
U	0.60	4.70	2	1.35	1.47	0.72	1.00	−0.69
Au	0.10	0.70	0.24	0.20	0.17	0.71	1.72	4.55
Th	0.60	17.80	7.18	6.45	5.65	0.79	0.89	−0.05
Sr	1.00	468.00	73.42	23.00	132.62	1.81	2.84	8.42
Cd	0.10	1.10	0.30	0.20	0.30	1.02	1.98	4.39
Sb	0.40	24.30	5.43	1.65	8.47	1.56	1.95	2.42
Bi	3.20	104.60	33	22.40	34.02	1.03	1.82	2.14
V	18.00	147	83	85.50	46.05	0.55	0.00	−1.36
Ca	700	21,000	3333	1550	5635	1.69	3.31	11.21
P	50	1280	470.83	395	351.14	0.75	1.21	1.51
La	2.60	60.60	19.57	16	14.74	0.75	2.13	5.81
Cr	4.00	153.00	57.25	51	42.00	0.73	1.02	1.12
Mg	1200	28,900	11,500	10,450	9718	0.85	0.55	−0.97
Ba	6	382	109	95	106	0.97	1.80	3.49
Ti	140	3340	1593	1570	981	0.62	0.35	−0.82
Al	2300	85,300	35,617	35,550	27,911	0.78	0.43	−1.02
Na	80	3150	1051	725	902	0.86	1.45	1.62
K	200	18,500	3383	1700	4934	1.46	3.05	9.92
W	0.40	6.60	4.23	4.95	2.15	0.51	−0.66	−1.13
Zr	4.90	110.40	59.33	52.30	37.33	0.63	0.06	−1.50
Ce	5	118	41	36	28.84	0.71	1.85	4.70
Sn	0.80	7.60	4.29	4.55	1.99	0.46	−0.16	−0.38
Y	1	8.60	5	4.70	2.47	0.49	0.04	−1.18
Nb	0.50	11.60	5.13	5.35	3.03	0.59	0.51	0.66
Ta	0.05	0.80	0.35	0.40	0.21	0.60	0.35	0.43
Be	1.00	1.00	1.00	1.00	0.00	0.00		
Sc	0.50	13.00	6.96	7.50	4.69	0.67	−0.03	−1.84
Li	4.10	44	17.18	11.40	13.03	0.76	0.90	−0.15
S	2000	96,000	41,167	30,000	29,905	0.73	0.52	−0.50
Rb	0.70	43.90	11.13	7.35	11.89	1.07	2.08	5.32
Hf	0.10	3.30	1.67	1.45	1.08	0.65	0.31	−1.13

VC = variation coefficient; SD = standard deviation (geochemical data are expressed in mg/kg).

2011; Martínez, 2002). According to the EDA results and the calculated statistical parameters, the Kettara soil involves different intervals of concentrations, which imply the existence of multiple populations resulting from geogenic and anthropogenic enrichment.

High concentration levels were found also for selected elements in the Kettara mine wastes (Table 2). The concentrations ranged between 879 and 6971 mg/kg for Cu, between 7 and 778 mg/kg for Pb, between 79 and 361 mg/kg for Zn, between 13 and 715 mg/kg for As and between 90,200 and 413,600 mg/kg for Fe. The mean concentrations are: Cu (2428 mg/kg), Pb (156 mg/kg), Zn (176 mg/kg), As (200 mg/kg), and Fe (294,825 mg/kg). These concentrations exceed widely the Clarke values given by McLennan (2001) indicating that Kettara mine wastes are extremely enriched in toxic elements. Consequently, it is plausible

Table 3
Theoretical semi-variogram model values and error estimation.

Element	Nugget	Number of lag	Root-mean-square	Average-standardized errors	Mean standardized	RMSE
Cu	0	12	271.80	265.80	0.03056	0.9958
Pb	418.56	12	29.28	29.48	0.02168	0.9951
Zn	2648.70	12	59.18	59.48	0.02974	0.9990
As	0	12	21.72	23.04	0.04592	0.9485
Fe	0	12	40,550	50,690	0.02712	0.7984

that the mine wastes are the main source of the soil contamination in Kettara region.

3.2. Determination of the soil geochemical background and anomalous values

The soil GB was defined based on the normality curves which provided a detailed visualization of experimental data distribution (Zhou and Xia, 2010). The plot curves of Cu, Pb, Zn, As, and Fe undergo an inflection point (Fig. 5a to e). The plot curves of Zn and Fe (Fig. 5c and e) show the existence of two populations of concentration. However, they show the existence of three populations of concentration for the other selected elements (Fig. 5a, b, and d). The inflection point allows distinguishing between natural or geogenic concentration values (the first population with low values) and anthropogenically influenced samples (second and third population with high values). The second and the third populations are interpreted as one population because they are representing the result of mining activity (Martínez et al., 2007). After deducting these two populations, the next step was to determine the GB values and the anomalous values for Kettara soils. From the studied variable, the values of the mean and medians for each population were derived. The mean values obtained for the first and for the second populations correspond, respectively, to the GB and to the anomalous values. Net anomalous values can be deduced by subtracting the GB values from the anomalous values.
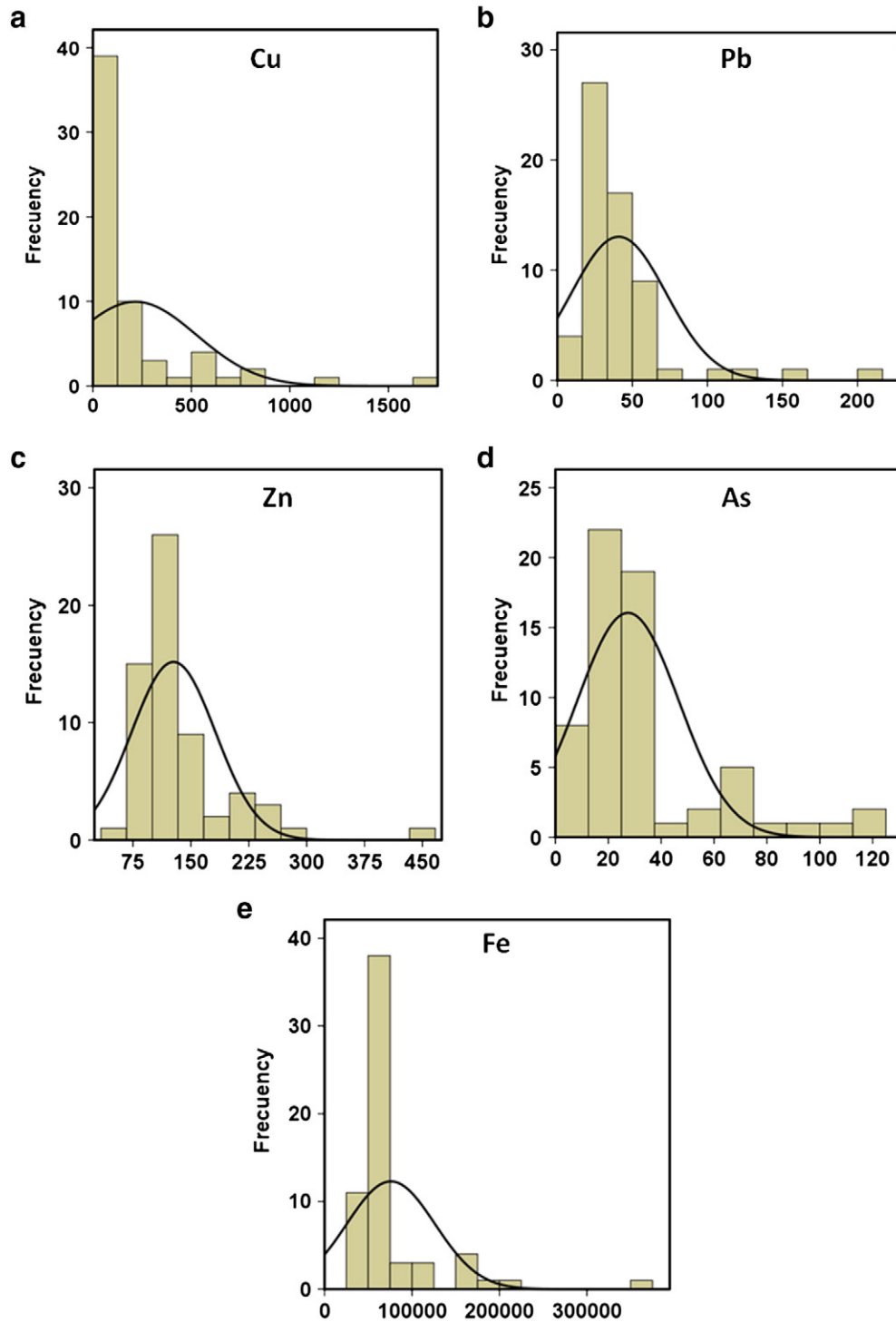
Fig. 3. Histograms and cumulative frequency curves for the selected elements in soil (concentrations are in mg/kg).

Soil GB values, anomalous values and net anomalous values are reported in Table 4. Unfortunately, in Morocco no environmental guidelines exist to regulate maximum permissible metals and metalloid concentrations in soils or to give reference values above which action should be taken to mitigate environmental risk. Therefore, the obtained values in this study will be compared with guidelines adopted by Canada and European community (CCME, 2006; Kabata-Pendias and Pendias, 1992). These guidelines were used in El-Khalil et al. (2008) research which were undertaken to assess the metal contamination from mining sites in the south of Morocco. The results indicate that GB values of Cu (43.8 mg/kg), Pb (21.8 mg/kg), Zn (102.6 mg/kg), and As (13.9 mg/kg) are bellow the used reference values (Table 4), whereas the GB of As exceeds slightly the Canadian guideline for As (12 mg/kg). According to these results, the geogenic concentrations of Cu, Pb, Zn, and As in Kettara soils will not have any adverse health effects. However, calculated anomalous values of Cu (397.2 mg/kg), Pb (55.6 mg/kg), Zn (196.5 mg/kg), As (42.6 mg/kg), and Fe (152,346 mg/kg) reveal the contribution of anthropogenic activity in contaminating Kettara soils. The
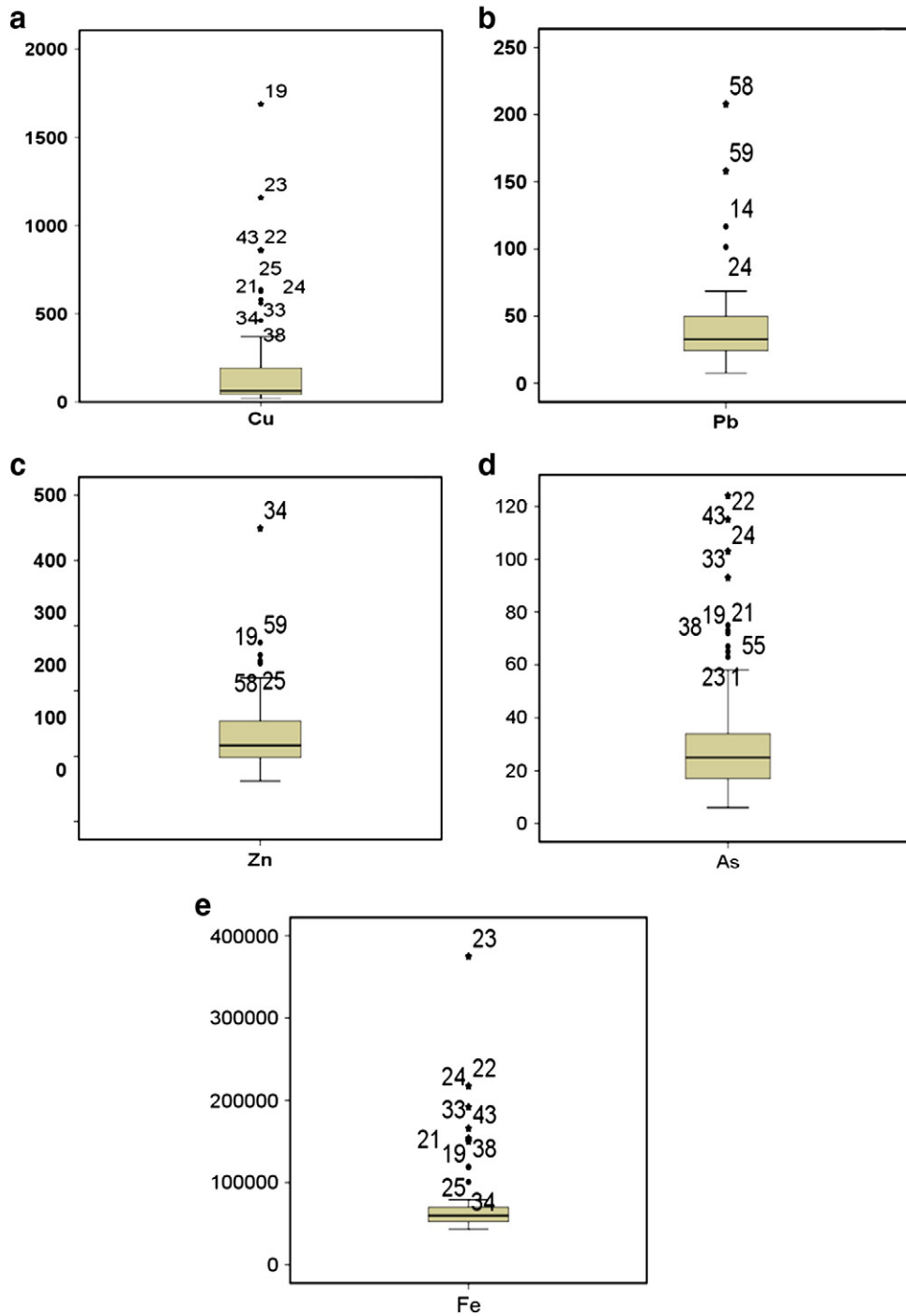
Fig. 4. Box plots for the concentration of selected elements in soil (concentrations are in mg/kg).

calculated anomalous values of Cu and As are above the used reference values (Table 4). The origin of anthropogenic activity and dispersion mechanism of contaminants will be discussed in the following section.

3.3. Geochemical mapping and multi-criteria analysis

The spatial distribution of metals and metalloid in the Kettara soils was analyzed using GIS mapping technique based on geostatistics (simple kriging). The obtained geochemical maps were then overlaid with other thematic maps such as stream networks and mine waste maps. According to the geochemical maps (Fig. 6), higher concentrations of Cu, Pb, Zn, As, and Fe were observed around and especially downstream of the mine wastes. These concentrations decreased with

increasing distances from the mine waste sites. Generally, areas located downstream of the mine wastes contained higher concentrations than those located upstream.

The studied Kettara soils are characterized by very high concentration levels of Cu ranging from 20 to 1687 mg/kg (Fig. 6a). Normal values are located essentially upstream of the mine wastes. The highest values which exceed widely the established GB (43.8 mg/kg) are located downstream of the mine wastes. Intermediate values are located far from the mine wastes downstream these letters. The geochemical map of Cu (Fig. 6a) showed that this element was derived essentially from the mine wastes located in the northern side of the study area and that was related to the second and third phases of the mining exploitation (mine wastes from the exploitation of pyrite and pyrrhotite).
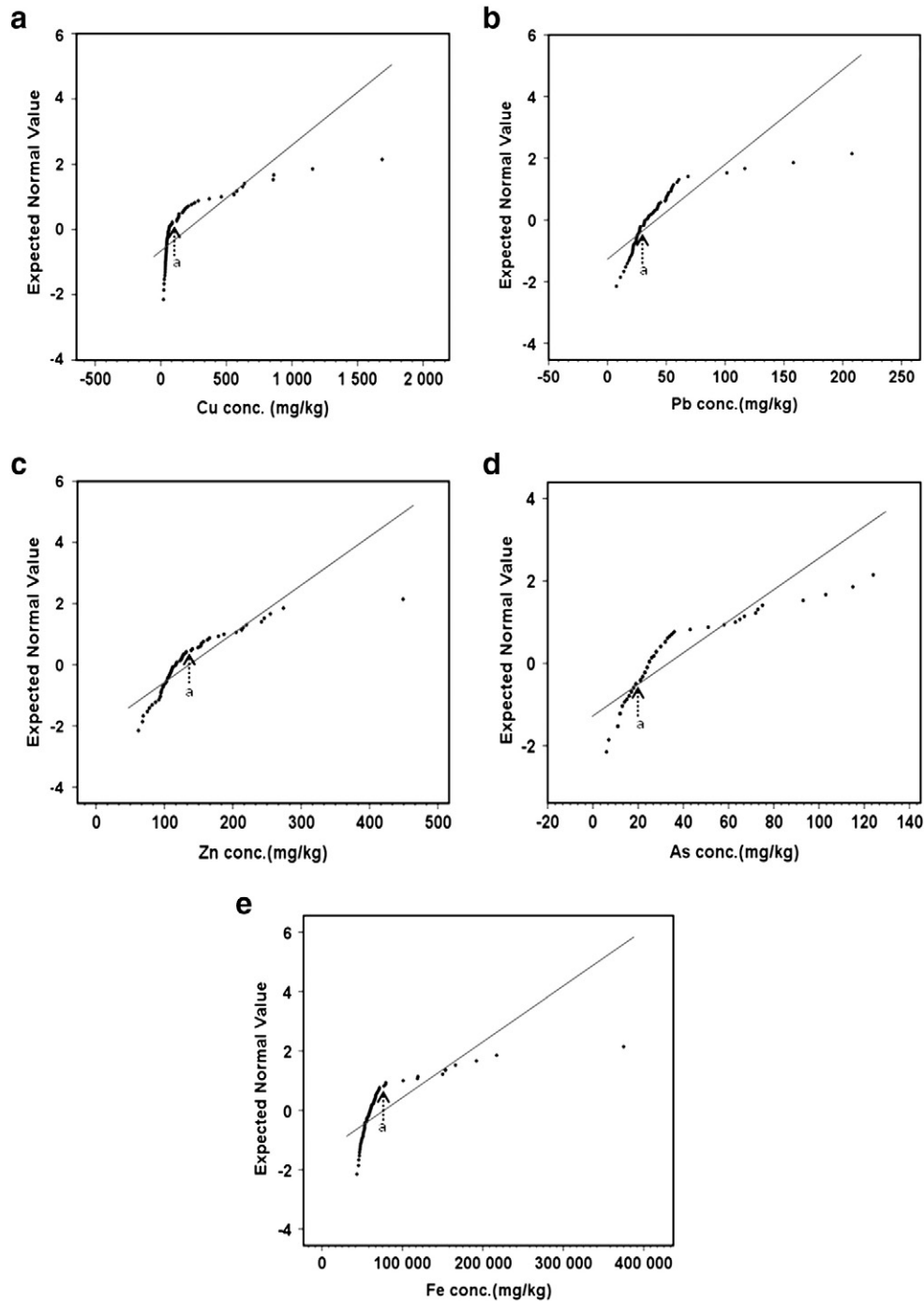
Fig. 5. Normal Q–Q plots for selected elements (arrow a: inflection point).

Those mine wastes are very rich in Cu (Table 2). The origin of Cu in the mine wastes was chalcopyrite (Hakkou et al., 2008a) which was present in the mineral paragenesis of Kettara (Hibti et al., 1999). This element was derived from the mine wastes by AMD action and subsequently dispersed with ephemeral water courses and surface runoff during the rainy season. It should be mentioned that the effect of the main flow direction of surface water follows slopes which enhance the pollution spread. Mechanical dispersion by wind action may play part especially if we know that prevailing wind flow has relatively the same direction of metallic dispersion.

Furthermore, Pb is characterized by moderate concentration values ranging from 7.6 to 207.8 mg/kg (Fig. 6b). Uncontaminated areas are located upstream of the Kettara mine wastes. Contaminated areas where

concentrations exceed the established GB (21.8 mg/kg) occur only in the vicinity of mine wastes located in the northern side of the study site. However, intermediate Pb concentrations are located in areas downstream of the mine wastes deposited in the southern side. After a review of Pb concentrations in mine waste samples, it was found that mine wastes located in southern part of the study site which were related to the first phase of mining exploitation (wastes from exploitation of iron oxide) contain lower Pb concentrations than those located in northern part. This explains the location of the formed hot-spots of Pb. This element was leached from the galena contained in the mine wastes by AMD action. Galena was left in mine wastes during the mining exploitation in Kettara mine (Hakkou et al., 2008a). The derived geochemical map (Fig. 6b) shows that Pb was mainly dispersed with surface water

Table 4
Geochemical background values, anomalous and net anomalous values obtained for Kettara soils.

Elements	Kettara soils (Saghlef schists)			Geochemical background of Kettara soils (first population)			Anomalous content of Kettara soils (second and third populations)			Net anomalous values	Canadian soils quality guidelines[a]	World ranges in non-polluted soils[b]
	N	Mean	Median	N	Mean (a)	Median	N	Mean (b)	Median	(b − a)		
Cu	62	203.4	62.3	34	43.8	43.05	28	397.2	222.2	353.4	63	6–60
Pb	62	41.4	32.9	26	21.8	22.45	36	55.6	44.4	33.8	70	10–70
Zn	62	136.0	116.5	40	102.6	105	22	196.5	172.5	93.9	200	17–125
As	62	33.3	25	20	13.9	13.5	42	42.6	30	28.7	12	1–15
Fe	62	76,974	59,800	49	56,978	55,800	13	152,346	150,000	95,368	–	–

N is number of samples (all concentrations are expressed in mg/kg).
[a] Canadian soil quality guidelines (CCME, 2006).
[b] Kabata-Pendias and Pendias (1992).

through the ephemeral water courses and surface runoff and by mechanical dispersion through the wind.

Fig. 6c illustrates that Zn concentrations were ranging from 60 to 450 mg/kg. This map shows a big contrast in concentrations between areas located upstream of the mine wastes, where Zn concentrations are normal and inferior to the established GB (102.6 mg/kg) and those located downstream, where high soil contaminations occurred. The contaminated areas are represented by two hot-spots where concentration levels reach 450 mg/kg. Intermediate concentration levels are also observed in the vicinity of mine wastes. Zn is a relatively mobile element which can easily be released from mine wastes which contain Zn bearing minerals (e.g. sphalerite) by AMD action. Likewise, Cu, Pb, and Zn had the same dispersion mechanism that prevailed in the study area.

For As element, Fig. 6d shows relatively similar distribution pattern as Cu. As concentration levels are ranging from 6 to 124 mg/kg. For this element, low concentrations which are inferior to the established GB (13.9 mg/kg) are observed upstream of the mine wastes. However, high concentration levels of As are observed in the contaminated areas located downstream of the mine wastes. The concentrations in these areas exceed widely the established GB. The spatial distribution of As in the Kettara soil explains its anthropogenic origin that is the deposited mine wastes. These latter contain high concentration levels of As especially in mine wastes located in the southern part of the study area where the concentration can reach 715 mg/kg (Table 2). As was leached from mine wastes by AMD as a result of the weathering process, and then it was spread in the study area mainly by surface water and wind flow.

Comparatively to the other selected elements, Fe has the highest concentration levels in the study area (Table 1). These concentrations are ranging from 43,300 to 371,400 mg/kg (Fig. 6e). This is not only because Fe is a major element and it's quite abundant in earth crust, but also because it was one of the main elements exploited in the Kettara mine. Fig. 6e shows that Fe has, relatively, similar spatial distribution pattern as Cu and As. Uncontaminated areas are located upstream of the mine wastes. However, heavily contaminated areas where concentrations exceed widely the established GB (56,978 mg/kg) are located just downstream of the mine wastes. Generally, geochemical map shows that concentrations decrease with distance from the mine wastes. These latter are extremely rich in Fe with concentrations ranging from 90,200 to 413,600 mg/kg with an average of 294,825 mg/kg (Table 2). These results corroborate Hakkou et al.'s (2008a) research in the same study region where they used X-ray diffraction analysis which revealed that many Fe bearing minerals (e.g. pyrrhotite, pyrite, goethite, magnetite and jarosite) are contained with different proportions in the Kettara mine wastes. Like the previous elements, Fe was leached from mine wastes with AMD and afterwards, dissipated in the study area by dispersion mechanism based mainly on surface water during rainy season followed by wind flow action.

The final risk map of soil contamination of Kettara (Fig. 7) was derived from the elaborated geochemical maps using the spatial analyst of Arc GIS software. Heavily contaminated areas were extracted from each considered geochemical map (Cu, Pb, Zn, As and Fe), then they were overlaid with other thematic maps of the study area (stream networks, mine wastes and geological maps). The risk map of the contaminated soils highlights areas which must be remediated.

Fig. 7 showed clearly that areas located downstream of the mine wastes contain very high concentration levels of Cu (>300 mg/kg), Pb (>100 mg/kg), Zn (>300 mg/kg), As (>50 mg/kg), and Fe (>100,000 mg/kg). However, areas located upstream of the mine wastes are unaffected with anthropogenic activity. According to our final results (Fig. 7) and to the ground truth, heavily contaminated areas occurred in the core of Kettara village where the majority of population is living. The concentration levels of metals and metalloid in contaminated soils exceed the soil quality guideline values adopted by Canada and the European community (CCME, 2006; Kabata-Pendias and Pendias, 1992). Therefore, adverse effect on human health might be expected, especially on young children's health that has a higher absorption rate of metals and metalloids because of their active digestion systems. Past studies have revealed that human exposure to high concentrations of As causes severe skin cancer and hyperkeratosis (Chowdhury et al., 2000). They revealed also that Cu accumulation in the human tissues may lead to Wilson's disease which causes liver disease and multiple organ dysfunctions (Peplow and Edmonds, 2005). Furthermore, Pb toxicity can cause hematological, gastrointestinal, and neurological diseases, and nephropathy, abortion, stillbirth, and neonatal death (Lockitch, 1993). Finally, the inhalation and the overload of iron may lead to pulmonary siderosis and tissue damage as a result of oxidation stress damage (Edison et al., 2008; Gurzau et al., 2003).

4. Conclusions

The aim of this study was the assessment of extension and intensity of soil contaminations with toxic elements from the abandoned Kettara mine. Soils and mine wastes around the abandoned site were sampled and analyzed for 41 chemical elements (Mo, Cu, Pb, Zn, Ag, Ni, Co, Mn, Fe, As, U, Au, Th, Sr, Cd, Sb, Bi, V, Ca, P, La, Cr, Mg, Ba, Ti, Al, Na, K, W, Zr, Ce, Sn, Y, Nb, Ta, Be, Sc, Li, S, Rb and Hf). The soil contaminations were evaluated for the selected metals and metalloid elements (Cu, Pb, Zn, As and Fe) based on enrichment factor computing, geochemical background determining using exploratory data analysis, and geochemical mapping based on GIS and geostatistics.

The obtained results show that statistical techniques applied for processing geochemical data are very useful for identifying geochemical background values, and for discriminating between geogenic and anthropogenic concentrations in Kettara soils. Moreover, they show that GIS and geostatistics are valuable tools in elaborating geochemical maps and quantifying both intensity and extension of contaminants and therefore monitoring soil contaminations. Finally, elaboration of ultimate risk map of soil contamination, which identifies hot-spots of contaminants using spatial analysis, might be very useful in the remediation of Kettara soils.
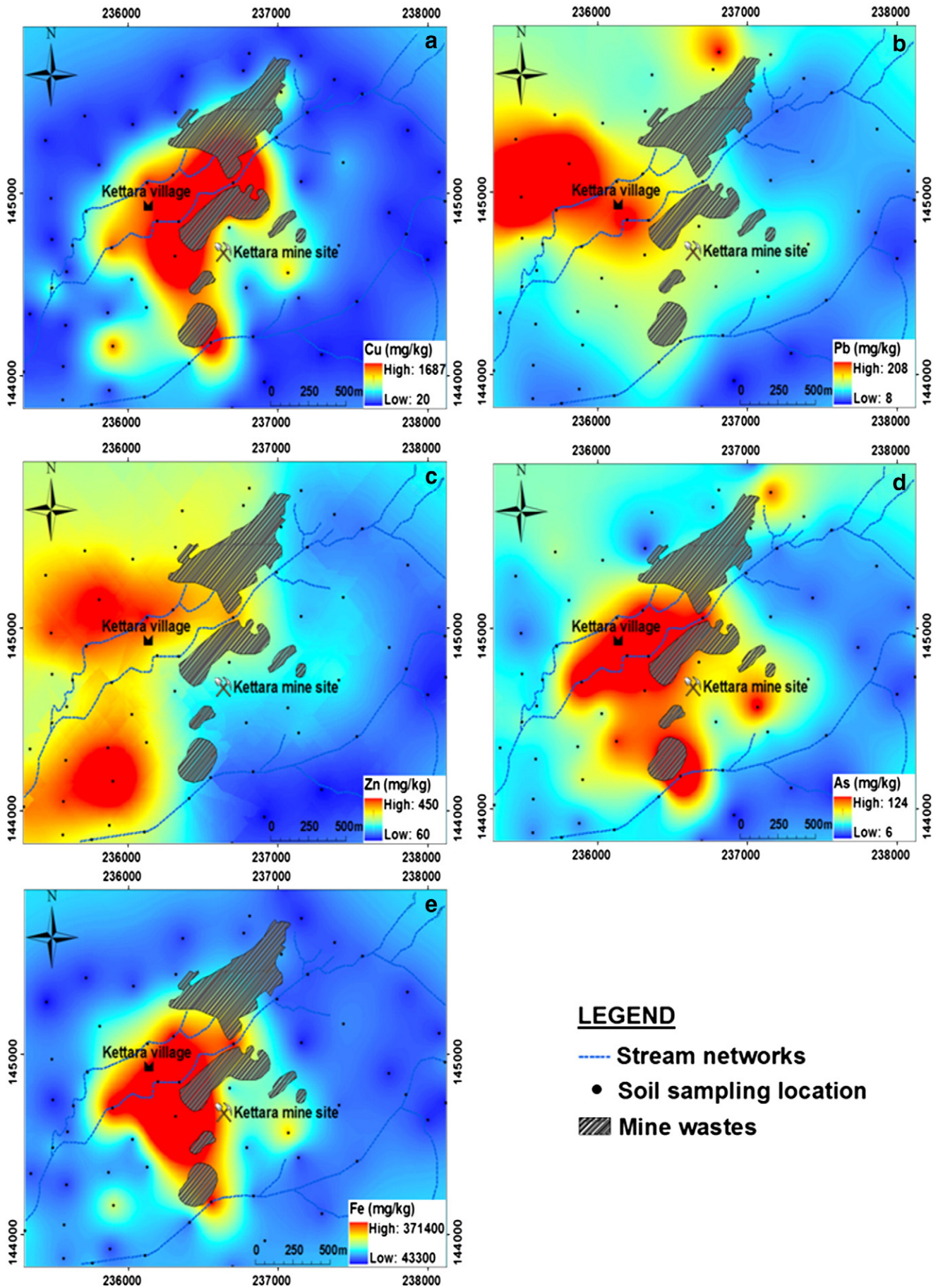
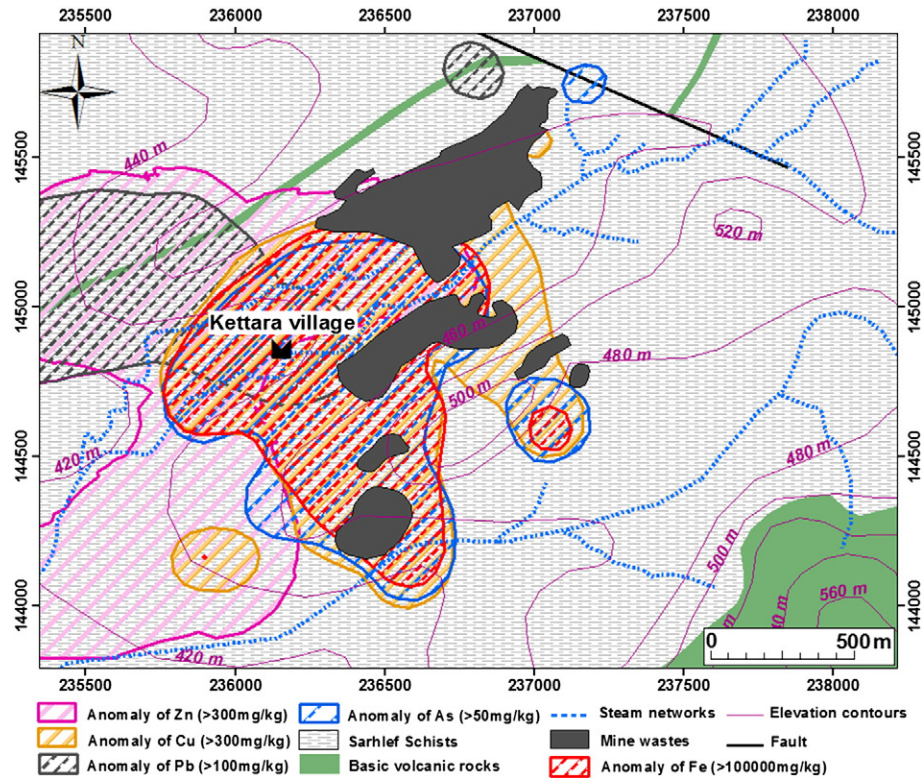**Fig. 6.** Geochemical maps of selected elements.

Fig. 7. Risk map of soil contamination with Cu, Pb, Zn, As, and Fe.

The concentration levels of Cu, As and Fe present in Kettara soils exceed the established geochemical background and the Canadian and European soil quality guidelines. Therefore, frequent adverse health effects might be expected. The derived geochemical maps show that: 1) most of the areas located downstream of the mine wastes are characterized by a very high concentration level of contaminants; 2) Kettara mine wastes are responsible for soil contaminations with metals and metalloid which were released by Acid Mine Drainage action; and 3) hydric dispersion pattern during a rainfall event is qualified as the main mechanism of contaminant spreading in the study area.

In order to assess soil pollution resulting from anthropogenic activity, the current study was undertaken in a limited and controlled area. This requires much time and high investment cost. In order to overcome this problem, in the second part of this research, we'll develop a new methodology integrating field spectroradiometric measurements, soil laboratory analyses, semi-empirical modeling, and remote sensing image processing in order to assess soil pollution and contaminations over a large territory with less time and investment.

The work conducted in this study can serve as the pre-work basis of establishing numerical models that could be used to simulate the realistic geochemical processes of the considered mine site in the future research.

References

Acosta, J.A., Faz, A., Martinez, M., Zornoza, R., Carmona, D.M., Kabas, S., 2011. Multivariate statistical and GIS-based approach to evaluate heavy metals behavior in mine sites for future reclamation. Journal of Geochemical Exploration 109, 8–17.

Albanese, S., Cicchella, D., De Vivo, B., Lima, A., 2007. Geochemical background and baseline values of toxic elements in stream sediments of Campania region (Italy). Journal of Geochemical Exploration 93, 21–34.

Bell, F.G., Donnelly, L.J., 2006. Mining and Its Impact on the Environment, First edition. Taylor and Francis Group, Oxon.

Bounessah, M., Atkin, B.P., 2003. An application of exploratory data analysis (EDA) as a robust non-parametric technique for geochemical mapping in a semi-arid climate. Applied Geochemistry 18, 1185–1195.

Bourennane, H., Douay, F., Sterckeman, T., Villanneau, E., Ciesielski, H., King, D., Baize, D., 2010. Mapping of anthropogenic trace elements inputs in agricultural topsoil from Northern France using enrichment factors. Geoderma 157, 165–174.

Buat-Menard, P., Chesselet, R., 1978. Variable influence of the atmospheric flux on the trace metal chemistry of oceanic suspended matter. Earth and Planetary Science Letters 42, 399–411.

Burgos, P., Madejón, E., Pérez de Mora, A., Cabrera, F., 2005. Spatial variability of the chemical characteristics of a trace-element-contaminated soil before and after remediation. Geoderma 130, 157–175.

Bussiere, B., 2009. Acid mine drainage from abandoned mine sites: problematic and reclamation approaches. Proceeding of International Symposium on Geo-environmental Engineering, ISGE2009, September 8–10, Hangzhou, China.

Cai, L., Xu, Z., Ren, M., Guo, Q., Hu, X., Hu, G., Wan, H., Peng, P., 2012. Source identification of eight hazardous heavy metals in agricultural soils of Huizhou, Guangdong Province, China. Ecotoxicology and Environmental Safety 78, 2–8.

Carlon, C., Critto, A., Marcomini, A., Nathanail, P., 2001. Risk based characterisation of contaminated industrial site using multivariate and geostatistical tools. Environmental Pollution 11, 417–427.

CCME, 2006. Canadian Soil Quality Guidelines for the Protection of Environment and Human Health. Canadian Council of Ministers of the Environment. (http://www.ccme.ca/ourwork/soil.html, Last accessed 2012-06-21).

Chen, J.Q., Wang, Z.X., Wu, X., Zhu, J.J., Zhou, W.B., 2011. Source and hazard identification of heavy metals in soils of Changsha based on TIN model and direct exposure method. Transactions of Nonferrous Metals Society of China 21, 642–651.

Chester, R., Stoner, J.H., 1973. Pb in particulates from the lower atmosphere of the eastern Atlantic. Nature 245, 27–28.

Chowdhury, U.K., Biswas, B.K., Chowdhury, T.R., Samanta, G., Mandal, B.K., Basu, G.C., Chanda, C.R., Lodh, D., Saha, K.C., Mukherjee, S.K., Roy, S., Kabir, S., Quamruzzaman,

Q., Chakraborti, D., 2000. Groundwater arsenic contamination in Bangladesh and West Bengal, India. Environmental Health Perspectives 108 (5), 393–397.

Cicchella, D., De Vivo, B., Lima, A., 2005. Background and baseline concentration values of elements harmful to human health in the volcanic soils of the metropolitan and provincial areas of Napoli (Italy). Geochemistry: Exploration, Environment, Analysis 5, 29–40.

Davies, T.C., Mundalamo, H.R., 2010. Environmental health impacts of dispersed mineralisation in South Africa. Journal of African Earth Sciences 58, 652–666.

Edison, E.S., Bajel, A., Chandy, M., 2008. Iron homeostasis: new players, newer insights. European Journal of Haematology 81, 411–424.

El-Khalil, H., El Hamiani, O., Bitton, G., Ouazzani, N., Boularbah, A., 2008. Heavy metal contamination from mining sites in South Morocco: monitoring metal content and toxicity of soil runoff and groundwater. Environmental Monitoring and Assessment 136, 147–160.

ESRI, 2012. Environmental Systems Research Institute. http://www.esri.com/software/arcgis (Last accessed 2012-07-19).

Ferguson, C., Kasamas, H., 1999. Risk Assessment for Contaminated Sites in Europe: Policy Framework, vol. 2. LQM Press, Nottingham NG7 2RD.

García-Lorenzo, M.L., Pérez-Sirvent, C., Martínez-Sánchez, M.J., Molina-Ruiz, J., 2012. Trace element contamination in an abandoned mining site in a semiarid zone. Journal of Geochemical Exploration 113, 23–35.

Giaccio, L., Cicchella, D., De Vivo, B., Lombardi, G., De Rosa, M., 2012. Does heavy metals pollution affects semen quality in men? A case of study in the metropolitan area of Naples (Italy). Journal of Geochemical Exploration 112, 218–225.

Guillén, M.T., Delgado, J., Albanese, S., Nieto, J.M., Lima, A., De Vivo, B., 2011. Environmental geochemical mapping of Huelva municipality soils (SW Spain) as a tool to determine background and baseline values. Journal of Geochemical Exploration 109, 59–69.

Guillén, M.T., Delgado, J., Albanese, S., Nieto, J.M., Lima, A., De Vivo, B., 2012. Heavy metals fractionation and multivariate statistical techniques to evaluate the environmental risk in soils of Huelva township (SW Iberian Peninsula). Journal of Geochemical Exploration 119–120, 32–43.

Gurzau, E.S., Neagu, C., Gurzaua, A.E., 2003. Essential metals—case study on iron. Ecotoxicology and Environmental Safety 56, 190–200.

Hakkou, R., Benzaazoua, M., Bussière, B., 2008a. Acid mine drainage at the abandoned Kettara mine (Morocco): environmental characterization. Mine Water Environment 27, 145–159.

Hakkou, R., Benzaazoua, M., Bussière, B., 2008b. Acid mine drainage at the abandoned Kettara mine (Morocco): 2. Mine Waste Geochemical Behavior. Mine Water Environment 27, 160–170.

Han, Y., Du, P., Cao, J., Posmentier, E.S., 2006. Multivariate analysis of heavy metal contamination in urban dusts of Xi'an, Central China. Sciences of the Total Environment 355, 176–186.

Hawkes, H.E., Webb, J.S., 1962. Geochemistry in Mineral Exploration. Harper.

Hibti, M., Bouabdelli, M., Mouttaqi, A., Sagon, J.P., 1999. L'effet du métamorphisme sur les minéralisations sulfurées de la province hercynienne (Meseta sud-occidentale, Maroc). Exemple des gisements sulfure's de Hajjar et de Kettara. Chronique Recherche Minière 536–537, 23–37.

Huvelin, P., 1977. Étude géologique et gîtologique du massif hercynien des Jebilotes (Maroc occidentale). Notes et Mémoires du Service Géologique du Maroc 232 bis.

Kabata-Pendias, A., Pendias, H., 1992. Trace Elements in Soils and Plants, second edition. CRC Press.

Khalil, A., Hanich, L., Hakkou, R., 2011. Development of an environmental database and a geographic information system on the abandoned mine of Kettara (Morocco). On the Proceedings of the Euro-Mediterranean Scientific Congress on Engineering, pp. 728–735 (ISBN13: 978-84-694-4025-4).

Komnitsas, K., Modis, K., 2006. Soil risk assessment of As and Zn contamination in a coal mining region using geostatistics. The Science of the Total Environment 371, 190–196.

Lghoul, M., Kchikach, A., Hakkou, R., Zouhri, L., Guerin, R., Bendjoudi, H., Teíxido, T., Penã, J.A., Enriqué, L., Jaffal, M., Hanich, L., 2012. Étude géophysique et hydrogéologique du site minier abandonné de Kettara (région de Marrakech, Maroc): contribution au projet de réhabilitation. Hydrological Sciences Journal 57 (2), 370–381.

Li, X., Feng, L., 2012. Multivariate and geostatistical analyzes of metals in urban soil of Weinan industrial areas, Northwest of China. Atmospheric Environment 47, 58–65.

Li, H.B., Lin, Z.H., Liu, S.X., 2001. Application of kriging technique in estimating soil moisture in China. Geographical Research 20 (4), 446–452.

Li, X., Lee, S.L., Wong, S.C., Shi, W., Thornton, I., 2004. The study of metal contamination in urban soils of Hong Kong using a GIS-based approach. Environmental Pollution 129, 113–124.

Lockitch, G., 1993. Perspectives on lead toxicity. Clinical Biochemistry 26, 371–381.

Lu, X., Wang, L., Lei, K., Huang, J., Zhai, Y., 2009a. Contamination assessment of copper, lead, zinc, manganese and nickel in street dust of Baoji, NW China. Journal of Hazardous Materials 161, 1058–1062.

Lu, X., Li, Loretta Y., Wang, L., Lei, K., Huang, J., Zhai, Y., 2009b. Contamination assessment of mercury and arsenic in roadway dust from Baoji, China. Atmospheric Environment 43, 2489–2496.

Martínez, J. 2002. Caracterización geoquímica y ambiental de los suelos en el sector minero de Linares. Ph.D. Thesis, Universidad Politécnica de Madrid, Madrid, Spain.

Martínez, J., Llamas, J., De Miguel, E., Rey, J., Hidalgo, M.C., 2007. Determination of the geochemical background in a metal mining site: example of the mining district of Linares (South Spain). Journal of Geochemical Exploration 94, 19–29.

Mclennan, S.M., 2001. Relationships between the trace element composition of sedimentary rocks and upper continental crust. Geochemistry, Geophysics, Geosystems 2 (ISSN: 1525-2027).

Nakayama, S.M.M., Ikenaka, Y., Hamada, K., Muzandu, K., Choongo, K., Teraoka, H., Mizuno, N., Ishizuka, M., 2011. Metal and metalloid contamination in roadside soil and wild rats around a Pb–Zn mine in Kabwe, Zambia. Environmental Pollution 159, 175–181.

ONEM (Observatoire Nationale de l'Environnement du Maroc), 1997. Monographie locale de l'environnement de la ville de Marrakech. Étude réalisée pour le compte de la Wilaya de Marrakech.

Peplow, D., Edmonds, R., 2005. The effects of mine waste contamination at multiple levels of biological organization. Ecological Engineering 24, 101–119.

Plant, J., Smith, D., Smith, B., Williams, L., 2001. Environmental geochemistry at the global scale. Applied Geochemistry 16, 1291–1308.

Reimann, C., Filzmoser, P., Garrett, R.G., 2005. Background and threshold: critical comparison of methods of determination. The Science of the Total Environment 346, 1–16.

Sams, J.I., Beer, K.M., 2000. Effects of coal-mine drainage on stream water quality in the Allegheny and Monongahela river basins—sulfate transport and trends. Water Resources Investigations Report 99-4208. Geological Survey, Lemoyne, Pennsylvania.

Sun, H., Li, J., Mao, X., 2012. Heavy metals' spatial distribution characteristics in a copper mining area of Zhejiang Province. Journal of Geographic Information System 4, 46–54.

U.S. Bureau of Mines, 1994. Proceedings of the International Land Reclamation and Mine Drainage Conference and 3rd International Conference on the Abatement of Acidic Drainage: U.S. Bureau of Mines. Special Publication, SP 06D-94.

Zhang, C.S., Selinus, O., Wong, P., 2000. Spatial structures of cobalt, lead, and zinc contents in tills in southeastern Sweden. GFF (Transactions of the Geological Society in Stockholm) 122, 213–217.

Zhang, C.S., Fay, D., Grath, D.M., Grennan, E., Carton, O.T., 2008. Statistical analyses of geochemical variables in soils of Ireland. Geoderma 146, 378–390.

Zhao, C., Hobbs, B.E., Ord, A., Peng, S., Mühlhaus, H.B., Liu, L., 2004. Theoretical investigation of convective instability in inclined and fluid-saturated three-dimensional fault zones. Tectonophysics 387, 47–64.

Zhao, C., Hobbs, B.E., Hornby, P., Ord, A., Peng, S., 2006. Numerical modelling of fluids mixing, heat transfer and non-equilibrium redox chemical reactions in fluid-saturated porous rocks. International Journal for Numerical Methods in Engineering 66, 1061–1078.

Zhao, C., Hobbs, B.E., Ord, A., Hornby, P., Peng, S., Liu, L., 2007. Mineral precipitation associated with vertical fault zones: the interaction of solute advection, diffusion and chemical kinetics. Geofluids 7, 3–18.

Zhao, C., Hobbs, B.E., Ord, A., 2008a. Convective and Advective Heat Transfer in Geological Systems. Springer.

Zhao, C., Hobbs, B.E., Hornby, P., Ord, A., Peng, S., Liu, L., 2008b. Theoretical and numerical analyses of chemical-dissolution front instability in fluid-saturated porous rocks. International Journal for Numerical and Analytical Methods in Geomechanics 32, 1107–1130.

Zhao, C., Hobbs, B.E., Ord, A., 2009. Fundamentals of Computational Geoscience: Numerical Methods and Algorithms. Springer.

Zhao, C., Hobbs, B.E., Ord, A., 2010a. Theoretical analyses of nonaqueous-phase-liquid dissolution induced instability in two-dimensional fluid-saturated porous media. International Journal for Numerical and Analytical Methods in Geomechanics 34, 1767–1796.

Zhao, C., Hobbs, B.E., Ord, A., 2010b. Theoretical analyses and numerical investigation into roles of geofluid flow in ore forming systems: integrated mass conservation and generic model approach. Journal of Geochemical Exploration 106, 251–260.

Zhao, C., Hobbs, B.E., Ord, A., 2012. Effects of domain shapes on the morphological evolution of nonaqueous-phase-liquid dissolution fronts in fluid-saturated porous media. Journal of Contaminant Hydrology 138–139, 123–140.

Zhou, X., Xia, B., 2010. Defining and modeling the soil geochemical background of heavy metals from the Hengshi River watershed (southern China): integrating EDA, stochastic simulation and magnetic parameters. Journal of Hazardous Materials 180, 542–551.

Zoller, W.H., Gladney, E.S., Duce, R.A., 1974. Atmospheric concentrations and sources of trace metals at the South Pole. Science 183, 199–201.